Continuously Variable Directional Couplers in Rectangular Waveguide*

M. E. BRODWIN†, MEMBER, IRE, AND V. RAMASWAMY‡, MEMBER, IRE

Summary—**Variable directional couplers can be constructed by placing a movable dielectric slab in the region of the coupling aperture. The coupling and directivity are a function of the position of the slab. For a two hole coupler, the change in coupling depends principally upon the variation of the field intensity at the coupling apertures. The directivity is solely a function of the difference in phase constants of the two waveguides. For a long slot narrow wall coupler, the coupling is a function of both intensity and phase variation. Some applications of this device to microwave measurements are described.**

I. Introduction

THE PROPERTIES of directional couplers can be simply controlled by varying the amplitude of the excitation of the coupling aperture and by changing the difference between phase constants of the main and auxiliary waveguides. These results can be easily achieved by moving a dielectric slab in one of the wave guides as shown in Fig. 1. This method of changing the parameters of the coupler is particularly advantageous since the controlling element, the dielectric slab, is noncontacting and therefore should not exhibit contact noise and should be capable of high power operation. It has been found, that by suitable design, the coupling can be increased or decreased, the directivity can be reduced to zero, and the preferred direction reversed.

An experimental and theoretical study for two common couplers, the narrow wall two hole and long slot couplers, has been performed. Typical results for the two hole coupler show a change in coupling of 30 db, equal power splitting between the two directions of the auxiliary arm, and reversal of the preferred direction of power flow. For the long slot side wall coupler, the coupling was varied from about −3 db to −12 db while the directivity was changed from −20 db through 0 db (equal power division) to +4 db (reversed direction).

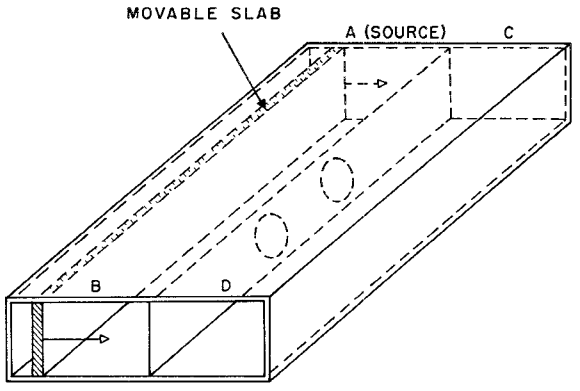

Fig. 1—Geometry of the variable directional coupler.

A theoretical analysis of the two hole coupler indicates that the coupling is determined primarily by the variation of field intensity at the aperture. Phase variation in the main waveguide produces only a minor effect upon coupling. The directivity of the two hole coupler depends solely upon the phase variation, provided that the coupling through each hole is the same. Thus the effects are both related to the movement of the slab but can be made somewhat independent. In the long slot coupler, the variation of both field intensity and phase contribute to the change in coupling and directivity.

In this paper, we shall present the experimental results and theoretical analyses of the variable two hole and long slot couplers and will describe some possible applications of these devices.

II. The Two Hole Narrow Wall Coupler

A series of X-band measurements were made with a variety of slab widths and dielectric constants. With polystyrene slabs, the coupling and directivity were determined for widths of 0.053, 0.10, and 0.21 in. A high dielectric constant material, $\epsilon_r = 15$, with a thickness of 0.05 in was also tested. The results for a low dielectric constant slab are shown in Fig. 2. As the slab is moved away from the side wall, the coupling increases from −21.5 db to a maximum of −23.5 db. In this region the directivity decreases rapidly from −37 db to −20 db. As the slab is moved closer to the aperture, the coupling decreases again and the directivity increases. Close to the aperture the coupling is significantly less than in the initial position. The data for thicker slabs show essentially the same trend except that the variation in coupling is increased. For the 0.10-in slab, the total change in coupling is 6.6 db and for the 0.21-in sample, the change is 11.4 db. The minimum directivity decreases with slab thickness. For example, with the 0.10-in slab, the directivity decreases to −14 db, and with the 0.21-in slab to −9 db.

When the permittivity is increased to $\epsilon_r = 15.0$ (Fig. 3), the shape of the curves is approximately the same,

* Received September 20, 1962; revised manuscript received November 30, 1962. This work was co-sponsored by a Walter P. Murphy Fellowship and by the Advanced Research Projects Agency through the Northwestern University Materials Research Center.

† Department of Electrical Engineering, Northwestern University, Evanston, Ill.

‡ Zenith Radio Corporation, Chicago, Ill. Formerly with Northwestern University.

but the characteristics of the coupler are altered. Initially the coupling increases and the directivity decreases until $d/b=0.18$. At this point, the directivity is zero and equal power is transmitted in both directions of the auxiliary waveguide with a coupling of -34 db. As the slab is moved farther toward the center to about $d/b=0.25$, the preferred direction is reversed and the junction behaves as a reversed coupler with $C=-40$ db and $d=+5$ db. In this manner, the device operates as a controllable power divider and power sampler.

The theoretical analysis consists of determining the equations for coupling and directivity. The expression for the coupling contains terms related to the excitation of the holes and the phase constants in the main and auxiliary waveguides. The directivity, however, depends solely upon the phase constants. The coupling equation is developed by considering two noninteracting coupling holes spaced a distance L between centers, and a nondirectional coupling constant k. The ratio of the coupled field to the field in the main waveguide is

$$C = -20\log_{10}\left[k\cos\frac{(\beta_1-\beta_2)L}{2}\right]^{-1} \quad (1)$$

where $\beta_{1,2}$ are the phase constants in the two waveguides. The coupling constant k is assumed to be proportional to the unperturbed field intensity at the point of coupling. In the case of narrow wall couplers, the field is the tangential magnetic field at the wall. The desired relation however, is the change in coupling produced by the variation in the position of the slab or

$$\Delta C = 20\log_{10}\left[k_0\left(\frac{H_{zs}}{H_{z0}}\right)\right] + 20\log_{10}\left[\cos\frac{(\beta_1-\beta_2)L}{2}\right] \quad (2)$$

where k_0 is the coupling constant with the slab removed from the waveguide. This constant is multiplied by the ratio of the field with the slab H_{zs} to the field without the slab H_{z0}. As the position of the slab is changed, the contribution to the change in coupling is 20 Log_{10} (H_{zs}/H_{z0}). The ratio is calculated by means of the theory outlined in Appendix I and is given by (12). The phase constant for the loaded waveguide β_1 is also presented in the same Appendix (5). The calculated

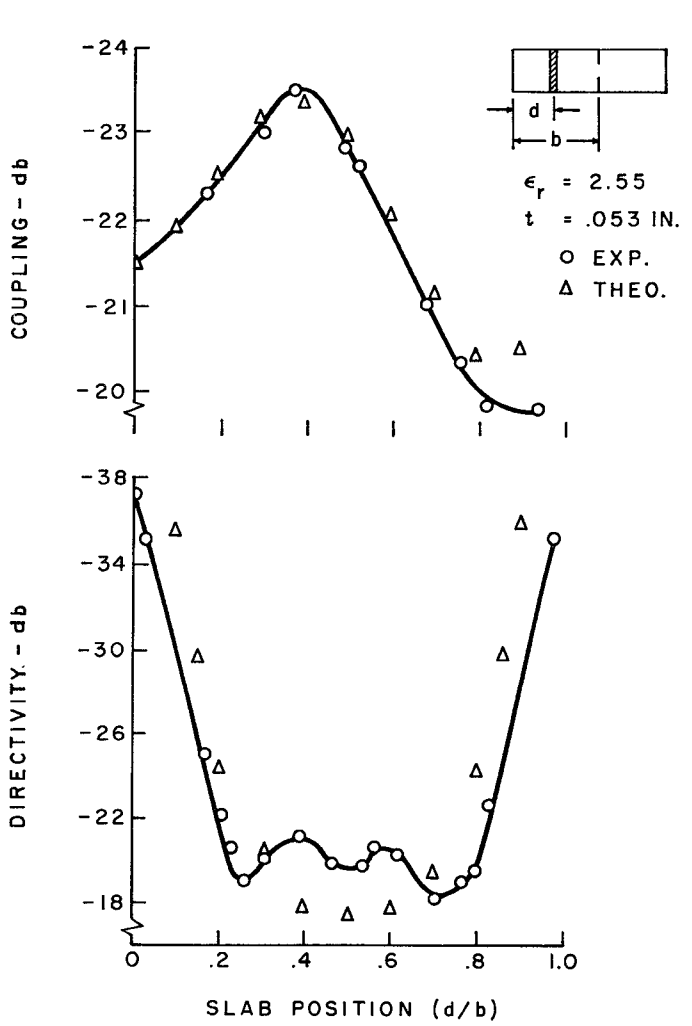

Fig. 2—The two hole coupler with a low permittivity slab.

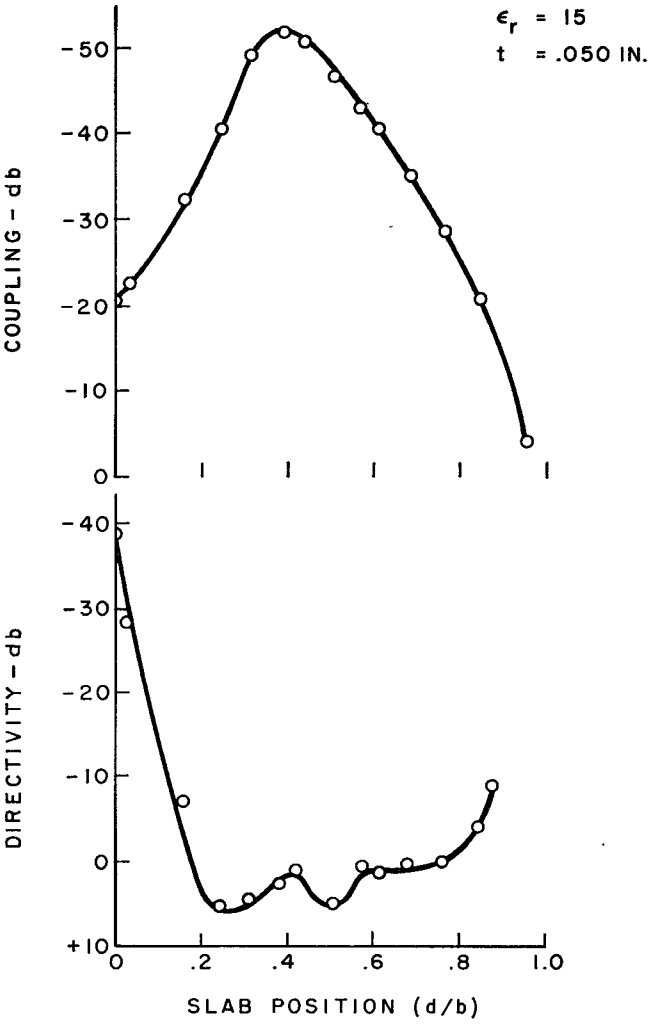

Fig. 3—The two hole coupler with a high permittivity slab.

values of the change in coupling are presented on Fig. 2.

The directivity is obtained by summing the fields in the reverse direction in the auxiliary guide and then forming the ratio of field magnitudes in the forward to reverse directions.

$$d = 20 \log_{10} \left[\frac{\cos (\beta_1 - \beta_2) L/2}{\cos (\beta_1 + \beta_2) L/2} \right]. \quad (3)$$

The directivity does not contain the coupling factor and thus the result is independent of the field intensity at the wall.

The theoretical points in Fig. 2 show excellent agreement for the coupling and reasonable agreement for the directivity. Another experimental result is that the minimum directivity decreases as the slab thickness is increased. This effect is explained by noting that the variation in β_1 increases as the slab thickness is increased and thus the directivity of the thicker slabs is decreased.

The experimental technique was chosen according to the range of the observed coupling and directivity. In all cases, the coupling was measured by placing a matched detector on the appropriate auxiliary port and using the detected signal level as a reference. The detector was then placed on the input waveguide and a precision attenuator adjusted to obtain the same level. For low directivity, $D < -10$ db, the same technique was employed. For high directivity, the variable load method of Schafer and Beatty [7] was used.

III. The Long Slot Narrow Wall Coupler

To examine the behavior of a 3-db coupler with variable excitation and phase, a long slot coupler was tested with differing thicknesses of polystyrene. The results for two thicknesses are shown in Figs. 4 and 5. In Fig. 4, the 0.053 in thickness, the initial coupling is -2.75 db. As the slab is moved toward the aperture, the coupling decreases to a minimum value of -0.75 db and then increases again. At this point, the directivity has been increased from an initial value of -11 db to -25.5 db. The directivity then decreases as the slab is moved toward the aperture. When the thickness was increased to 0.10 in (Fig. 5) the same qualitative results were obtained except that range of variation in the parameters is increased and the preferred direction of power flow is reversed.

The analysis of the coupling as a function of slab position is developed by means of coupled mode theory for the tightly coupled case (Appendix II). The magnitude of the field in the auxiliary arm is given by (15).

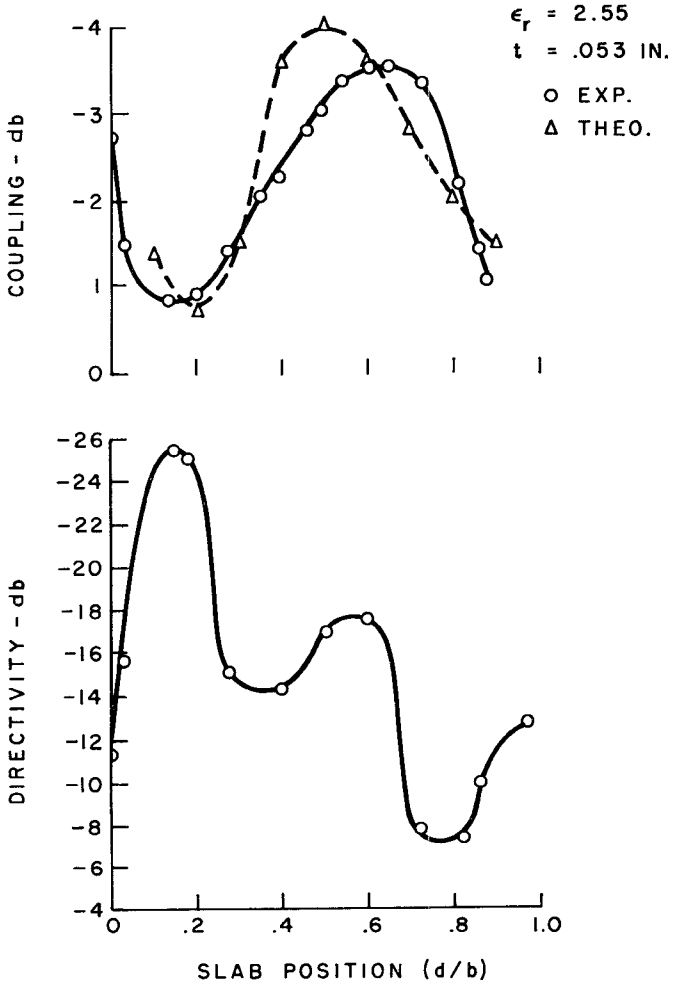

Fig. 4—The long slot side wall coupler with a thin slab.

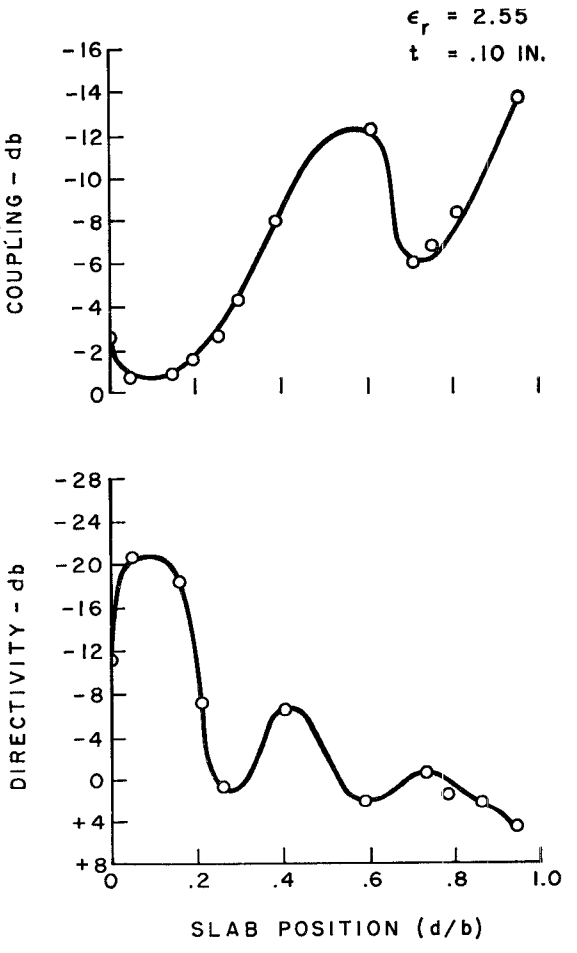

Fig. 5—The long slot side wall coupler with a thick slab.

$$|E_2| = \frac{2C}{[(\beta_1 - \beta_2)^2 + 4C^2]^{1/2}} \cdot \sin\left\{\frac{[(\beta_1 - \beta_2)^2 + 4C^2]^{1/2}}{2} x\right\}$$

where C is a coupling parameter assumed to vary as H_{zs}/H_{z0} and x is the effective length of the slot. The results of a calculation of the change in coupling due to field intensity and phase constant variation is shown in Fig. 4. Note that the qualitative agreement is fairly good but that the quantitative agreement is weak. We have not been able to find a satisfactory explanation for the discrepancy.

IV. Conclusion

The principal results of this investigation of variable directional couplers depend upon the type of coupling mechanism. In general, the coupling is a function of both field intensity and phase constant. For the two hole coupler, the variation in field intensity is the principal cause of the change in coupling. Both effects are equally important for the coupling variation in the long slot coupler. In the two hole coupler, directivity depends solely upon the difference in phase constants. For those apertures analyzed by means of the tight coupled mode theory, the directivity cannot be predicted. Experimentally the directivity exhibits a decreasing trend with the movement of the slab; a trend which is accelerated by increasing slab thickness.

Continuously variable two hole couplers can therefore be designed with almost independent control of coupling and directivity, since coupling depends primarily upon the excitation of the apertures and directivity upon the difference in phase constants. For example, a calculation of the change in coupling due to the change in phase constant of the coupler in Fig. 2 shows an expected variation of 0.09 db whereas the field intensity variation yields a result of 3.0 db. For coupled mode devices, coupling and directivity are more closely related and trial designs are required to determine the feasibility of a given specification.

The results of this study are also applicable to the analysis of ferrite controlled couplers as described by Fox, Miller, and Weiss [8]. In the reported work, only the difference in phase constants is considered whereas the results with dielectric slabs show that field intensity variation may be more important in affecting the coupling than the phase variation.

Applications of continuously variable directional couplers include: easily varied samplers for in-line tests of microwave apparatus, power dividing and switching. A more unique application is in the development of reflectometers. For example, one form of simple reflectometer can be constructed by switching the output of one of the auxiliary arms to a crystal detector, amplifying the signal and servoing the slab to a null position. An analysis shows that this position of the slab corresponds to a directivity which is equal to the reflection coefficient of the load placed upon the main arm. Another possible application is to apply the phase dependence of the directivity of the two hole coupler to maximize the directivity at any frequency in the operating band.

Appendix I

Phase Constant and Field Distribution for the Slab Loaded Rectangular Waveguide

A number of analyses of this structure have been published. Woodward [1] derived exact expressions for the propagation constant and field distribution of a symmetrically located slab. Montgomery, Dicke, and Purcell [2] presented the propagation constant as a function of slab thickness for both symmetric and asymmetric slabs. Vartanian, Ayres, and, Helgesson [3] discussed the symmetrically located slab from the viewpoint of increased bandwidth and power capability. An approximate method was outlined by Berk [4] using variational principles.

The information required for the variable directional coupler is the phase and field intensity as a function of the position of the slab. We have derived exact expressions but they are too complicated and require computer solution. A very simple approach to this problem for thin slabs was published by Ishida and Mushiake [5]. The essential point in their work is to consider the slab as a shunt admittance across the waveguide. Since the original paper is in Japanese, we shall outline the important steps in the development.

Consider a dielectric slab, of thickness t and length l, placed in a parallel plane structure as shown in Fig. 6.

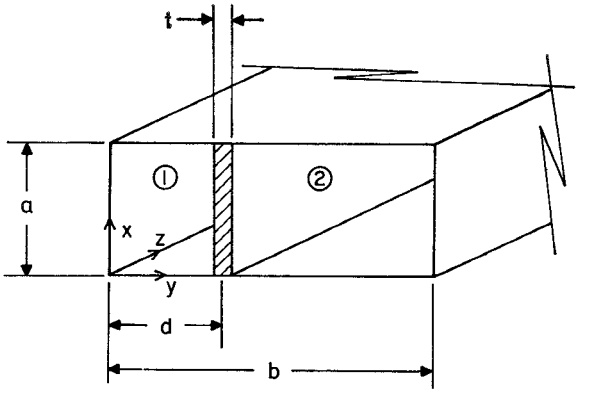

Fig. 6—Geometry of the slab loaded rectangular waveguide.

The height of the slab a is the same as the separation between the planes. The admittance is a pure imaginary (lossless dielectric) and is given by $\Delta I/V$. ΔI is the difference in displacement current caused by the presence of the slab. With slab in position, the displacement current is $jw\epsilon tlE$. In the absence of the slab, the current is $jw\epsilon_0 tlE$. The voltage V is Ea. The ad-

mittance per unit length is therefore

$$Y = jB = \frac{jw\epsilon_0(\epsilon_r - 1)t}{a}. \tag{4}$$

The implicit approximation is that the field is uniform throughout the transverse dimension of the slab. By means of this assumption, we need consider only the fields in the regions on either side of the slab.

The determinantal equation is found from the boundary conditions upon the fields at the slab. The assumed propagation term is of the form $e^{-\gamma h_z z}$ where $h_z = \beta - j\alpha$; β is the phase constant, and α, the attenuation constant. The scalar Helmholtz equation is therefore

$$\nabla_t^2 H_z + h_y^2 H_z = 0$$

and

$$h_z^2 = k^2 - h_y^2$$
$$k^2 = w^2\epsilon_0\mu_0. \tag{5}$$

The field equations in the regions denoted in Fig. 6 are

$$E_{x1} = jw\mu_0 h_y A_1 \sin h_y y$$
$$H_{y1} = jh_y h_z A_1 \sin h_y y$$
$$H_{z1} = h_y^2 A_1 \cos h_y y \tag{6}$$

and

$$E_{x2} = -jw\mu_0 h_y A_2 \sin h_y(b - y)$$
$$H_{y2} = -jh_y h_z A_2 \sin h_y(b - y)$$
$$H_{z2} = h_y^2 A_2 \cos h_y(b - y). \tag{7}$$

The boundary condition for these fields is that, at $y = d$,

$$E_{x1} = E_{x2} = E_x$$
$$H_{z2} - H_{z1} = E_x a Y. \tag{8}$$

The determinantal equation is found to be

$$h_y \frac{\sin h_y b}{\sin h_y(b - d) \cdot \sin h_y d} = -jw\mu_0 a Y.$$

Note that the eigenvalue h_y can be either real or imaginary, $h_y = \xi$ or $j\eta$. If we restrict our interest to real values and a lossless dielectric, the determinantal equation becomes

$$\frac{\xi b \sin \xi b}{\sin [\xi b(1 - (d/b))] \cdot \sin \xi b(d/b)} = w\mu_0 abB. \tag{9}$$

Curves of ξb vs $w\mu_0 abB$ for different slab positions, d/b, are graphed by Tetsuro and Yasuto [5]. Once the eigenvalue has been determined for a specific slab position, the phase constant can be found from (5).

The next problem is to determine how the field intensity H_z in the region of the coupling aperture, varies as the slab is moved across the waveguide. To do this we assume that the power flow in the slab loaded case is the same as in the empty waveguide. This equality leads to the ratio of the field intensities as a function of the position of the slab.

Let $P_{0,s}$ be the power flowing down the waveguide for the empty and slab loaded cases, respectively.

$$P_0 = C_0 A_0^2$$
$$P_s = C_s A_s^2 \tag{10}$$

where $C_{0,s}$ are the results of evaluating the integrals of the Poynting Vector over the cross section of the guide. From the field equations for the empty and slab loaded geometry,

$$H_{z0} = \xi_0^2 A_0$$
$$H_{zs} = \xi^2 \zeta A_s \tag{11}$$

where

$$\zeta = -\sin(\xi b)(d/b)/\sin(\xi b)(1 - (d/b)).$$

Upon equating the powers and solving for the ratio of the fields, we find that

$$\frac{H_{zs}}{H_{z0}} = \frac{\xi^2}{\xi_0^2}\zeta\sqrt{\frac{C_0}{C_s}} \tag{12}$$

where it can be shown that

$$\xi_0 = \frac{\pi}{b}, \qquad C_0 = \tfrac{1}{4}abw\mu_0\left(\frac{\pi}{b}\right)^2\beta_0$$

$$C_s = \tfrac{1}{4}aw\mu_0\xi\beta\left\{\xi d - \tfrac{1}{2}\sin 2\xi d + \frac{\xi(b - d)\sin^2 \xi d}{\sin^2 \xi(b - d)} - \sin^2 \xi d \cdot \cot \xi(b - d)\right\}.$$

By evaluating (12) for each position of the slab, the relative value of the field intensity at the coupling aperture can be determined.

Appendix II

Theoretical Coupling of the Long Slot Coupler

The coupling variation for this case was developed from the tight coupling theory of S. E. Miller [6]. The equations for the wave amplitude in the auxiliary waveguide are modified by the change in coupling produced by the variation in field intensity at the aperture.

The principal relations for the wave in the coupled waveguide, (22)–(24) of Miller [6], are

$$E_2 = \frac{k}{\sqrt{(\gamma_1 - \gamma_2)^2 + 4k^2}}(e^{r_1 x} - e^{r_2 x}) \tag{13}$$

where

$$r_{1,2} = \frac{-(\gamma_1 + \gamma_2 + 2k) \pm \sqrt{(\gamma_1 - \gamma_2)^2 + 4k^2}}{2} \tag{14}$$

and x is the effective length of the coupling aperture. For the case of the long slot coupler k the coupling

parameter is a pure imaginary, and there are no losses in either waveguide. Thus $k=jc$, $\gamma_{1,2}=j\beta_{1,2}$. Upon inserting these conditions and solving for the magnitude of the field in the auxiliary waveguide we find that

$$|E_2| = \frac{2C}{\sqrt{(\beta_1-\beta_2)^2+4C^2}} \cdot \sin\left(\frac{\sqrt{(\beta_1-\beta_2)^2+4C^2}}{2}x\right). \quad (15)$$

As the slab is moved across the main waveguide, both β_1 and C are affected. The phase constant is determined by means of (5) and the change in coupling is calculated in the following manner. With the slab at $d=0$, the two phase constants are equal and the coupling is found from $|E_2|=\sin C_0X$. For each subsequent position of the slab, C_0 is multiplied by the factor H_{zs}/H_{z0} given in (12).

References

[1] A. M. Woodward, "Transmission in waveguides," *Wireless Engr.*, vol. 24, pp. 192–196; July, 1947.

[2] C. G. Montgomery, R. H. Dicke, and E. M. Purcell, "Principles of Microwave Circuits," M.I.T. Rad. Lab. Ser., McGraw-Hill Book Co., Inc., New York, N. Y., vol. 8, pp. 385–389; 1948.

[3] P. H. Vartanian, W. P. Ayres, and A. L. Helgesson, "Propagation in dielectric slab loaded rectangular waveguide," IRE TRANS. ON MICROWAVE THEORY AND TECHNIQUES, vol. MTT-6, pp. 215–222; April, 1958.

[4] A. D. Berk, "Variational principles for electromagnetic resonators and waveguides," IRE TRANS. ON ANTENNAS AND PROPAGATION, vol. AP-4, pp. 104–111; April, 1956.

[5] I. Tetsuro, and M. Yasuto, "Universal solution of rectangular waveguide loaded with a dielectric slab," *J. Inst. Elec. Commun. Engrs., Japan*, vol. 43, pp. 943–947; September, 1960.

[6] S. E. Miller, "Coupled wave theory and waveguide applications," *Bell Sys. Tech. J.*, vol. 33, pp. 661–719; May, 1954.

[7] G. E. Schafer and R. W. Beatty, "A method for measuring the directivity of directional couplers," IRE TRANS. ON MICROWAVE THEORY AND TECHNIQUES, vol. MTT-6, pp. 419–422; October, 1958.

[8] A. G. Fox, S. E. Miller, and M. T. Weiss, "Behavior and applications of ferrites in the microwave region," *Bell Sys. Tech. J.*, vol. 34, pp. 5–103; January, 1955.

Millimeter Wavelength Resonant Structures*

R. W. ZIMMERER†, MEMBER, IRE, M. V. ANDERSON†,
G. L. STRINE†, AND Y. BEERS†, MEMBER, IRE

***Summary*—This paper discusses the construction of millimeter wave Fabry-Perot resonators, using both planar and spherical reflectors. It also discusses the equivalent circuits of planar reflectors and the method of obtaining efficient power transfer into the resonators.**

THIS PAPER is a further report on the work on millimeter wave Fabry-Perot interferometers that was started in this laboratory by Culshaw.[1–5] These interferometers have become of wide interest because of their use as resonators in optical and millimeter wave masers. These resonators have many other potential uses as spectrometers, refractometers, and wave meters.

* Received October 23, 1962; revised manuscript received November 30, 1962. A condensed version of this paper was presented at the PGMTT National Symposium in Boulder, Colo., on May 22, 1962.

† Radio Standards Laboratory, National Bureau of Standards, Boulder, Colo.

[1] W. Culshaw, "Reflectors for a microwave Fabry-Perot interferometer," IRE TRANS. ON MICROWAVE THEORY AND TECHNIQUES, vol. MTT-7, pp. 221–228; April, 1959.

[2] W. Culshaw, "High resolution millimeter wave Fabry-Perot interferometer," IRE TRANS. ON MICROWAVE THEORY AND TECHNIQUES, vol. MTT-8, pp. 182–189; March, 1960.

[3] W. Culshaw, "Resonators for millimeter and submillimeter wavelengths," IRE TRANS. ON MICROWAVE THEORY AND TECHNIQUES, vol. MTT-9, pp. 135–144; March, 1961.

[4] W. Culshaw, "Millimeter wave techniques," *Advances in Electronics and Electron Phys.*, vol. 15, pp. 197–263; 1961.

[5] W. Culshaw, "Measurement of permittivity and dielectric loss with a millimetre-wave Fabry-Perot Interferometer," *Proc. IEE*, vol. 109, pt. B, Suppl. No. 23, pp. 820–826; 1961.

In the millimeter region the ratio of wavelength to the mirror dimensions, although small compared to unity, is much larger than in the optical region. Therefore, diffraction losses in the millimeter region tend to be much larger. At the same time modes are separated more widely, and it is usually possible to work with a single mode. In the optical region mirrors are made of semisilvered surfaces or by multilayered dielectric surfaces. As is well known,[6] with such mirrors large reflectivity is incompatible with low resonance transmission loss. Culshaw realized that in the millimeter region other techniques allowing the achievement of both objectives were practical. He evolved a scheme of drilling an array of holes in metallic sheets and started work with metal films with photoetched holes deposited on dielectric slabs. We have further developed this technique and have used thin perforated metal foils stretched on frames. This technique appears to be the best available for use with plane reflectors.

For many applications Fox and Li[7] and Boyd and Gordon[8] have demonstrated the superiority of con-

[6] M. Born and E. Wolf, "Principles of Optics," Pergamon Press, Inc., New York, N. Y., Sec. 7.6; 1959.

[7] A. G. Fox and T. Li, "Resonant modes in a maser interferometer," *Bell Sys. Tech. J.*, vol. 40, pp. 453–488; March, 1961.

[8] G. D. Boyd and J. P. Gordon, "Confocal multimode resonator for millimeter through optical wavelength masers," *Bell Sys. Tech. J.*, vol. 40, pp. 489–508; March, 1961.